Electronic Supplementary Information

Specific single-molecule detection of glucose in a supramolecularly designed tunnel junction

Tomoaki Nishino,[ab] Hiroshi Shiigi,[b] Manabu Kiguchi[a] and Tsutomu Nagaoka[b]

[a] Department of Chemistry, School of Science, Tokyo Institute of Technology, Ookayama, Meguro-ku, Tokyo 152-8551, Japan; [b] Department of Applied Chemistry, Graduate School of Engineering, Osaka Prefecture University, Sakai, Osaka 599-8570, Japan

CONTENTS

Conductance histograms for thiolated glucose and galactose

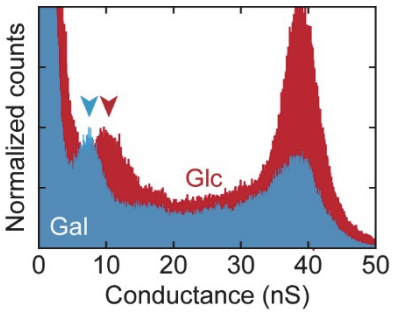

Fig. S1. The histogram was obtained from *I–z* measurements (bias voltage: 200 mV, initial set-point current: 7.5 nA) using the 4MPBA tip and Au surface modified with glucose (Glc, magenta) and galactose (Gal, cyan), and shows all of the measurable range of the preamplifier (1 nA/V). Bin size: 25 pS. The peaks near 40 nS were due to the initial set-point (7.5 nA, corresponding to 37.5 nS) at which the tip stayed for a short time (0.1 ms) before every *I–z* measurement.

pH dependence of molecular junction formation

We examined the pH dependence of the formation of the molecular junction between surface-tethered glucose and the 4MPBA tip because the interaction between boronic acid and saccharide is known to be highly dependent on solution pH.[1] Higher pH, at which most of the boronic acid exists in the anionic form, favors the binding of boronic acid with the diol of saccharide. In the present experiments, tunneling current was measured in the time domain (current–time, *I–t*, traces)[2,3] in acidic and basic pH conditions. After bringing the molecular tip very close to the sample surface, the tip position and tip–sample distance were maintained constant by freezing the feedback loop of STM, and the current was recorded as a function of time. When measurements were performed in a basic (pH 8.5) solution, the resulting *I–t* traces exhibited sudden current jumps and consecutive plateaus over the stable background set-point current (Fig. S2a). These jump−plateau signatures are ascribed to the formation of the molecular junction connecting the tip and substrate, which in turn induces electron transfer. The increased amount of the current relative to the set-point

current in the plateau regions was evaluated, and the conductance histogram was constructed on the basis of the increased value (Fig. S2b). The histogram was characterized by a single peak, and its position (8.2 nS, 1.1×10^{-4} G_0, where G_0 is the fundamental conductance quantum) reasonably agrees with that observed in the conductance histogram for *I–z* measurements (Fig. 1c, magenta). This result demonstrates that identical molecular junctions are formed in *I–t* and *I–z* measurements. The data recorded in the basic solution was statistically analyzed further by two-dimensional (2D) histograms (Fig. S2c), where the color scale represents the count number of the data point. For creating this histogram, the origin of the time axis was set at the beginning of the jump–plateau signatures, and each *I–t* plot was overlaid. Fig. S2c shows that the plateau, and thus the molecular junction, persists for up to approximately 0.2 s.

The same measurements were conducted in an acidic (pH 4.0) solution. Similar to those

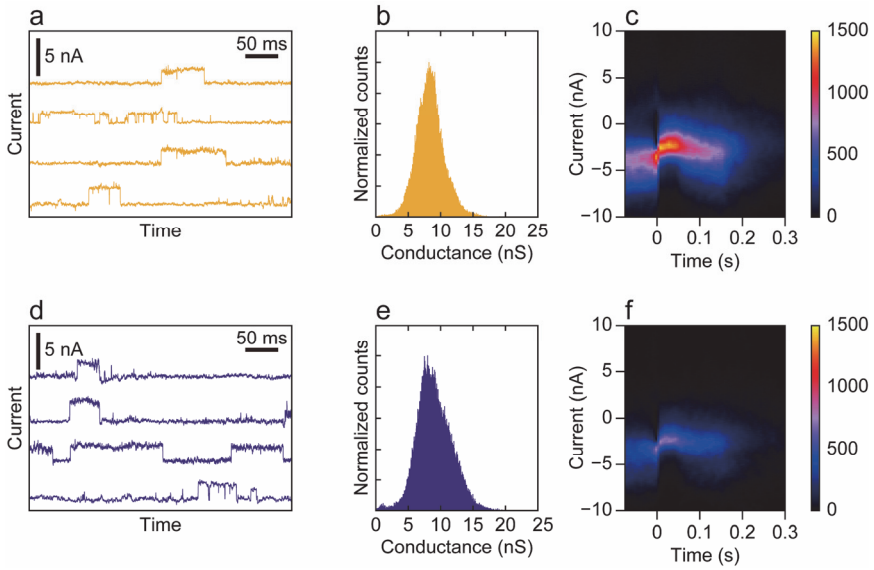

Fig. S2. Representative *I–t* plots measured in pH (a) 8.5 and (d) 4.0 buffer solutions. Bias voltage: 200 mV, set-point current: 5 nA. 1D conductance histograms for measurements in pH (b) 8.5 and (e) 4.0 solutions. Counts are normalized by the peak values (570 and 383 for pH 8.5 and 4.0, respectively). Bin size: 5 pA. 2D histograms for measurements in pH (c) 8.5 and (f) 4.0 solutions. The color scale represents the count number of the data point. Bin size in time and current axes: 1 ms and 5 pA, respectively.

observed in the basic solution, plateaus were observed in the *I–t* traces (Fig. S2d), and the peak appeared at 8.7 nS (1.1×10^{-4} G_0) in the conductance histogram (Fig. S2e). The peak position was consistent with those observed in both the *I–t* measurement in the basic solution and *I–z* measurement, demonstrating that similar molecular junctions are formed. In contrast, a notable difference was observed in the 2D histogram (Fig. S2f). Although the numbers of the 4MPBA tips used for the measurements and the measurement durations were the same in the basic and acidic solutions, the 2D histogram contained significantly less counts (intensity) for the acidic solution (Fig. S2f) than for the basic solution (Fig. S2c). In other words, the 2D histograms indicate that the probability of junction formation is notably higher in a basic milieu than in an acidic one. This observation is in agreement with the pH dependence for the binding of boronic acid with diol; thus, we attributed the formation of the molecular junction to the reversible covalent bond between the saccharide immobilized on the sample surface and the 4MPBA tip.

Conductance of glucose–4MPBA junction measured at different bias voltages

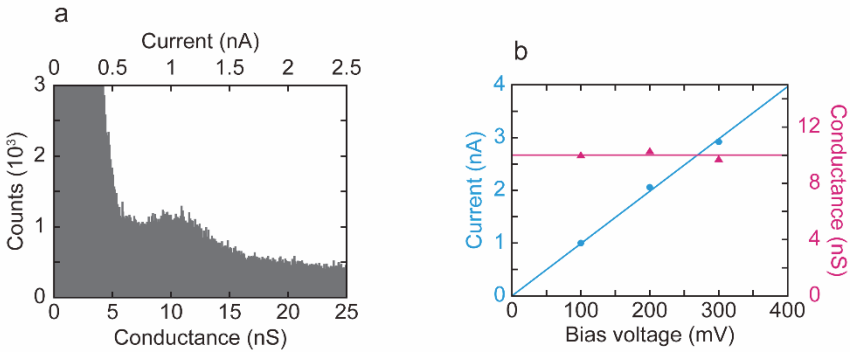

Fig. S3. (a) Conductance (current) histogram obtained from *I–z* measurements using the 4MPBA tip and Au surface modified with glucose. Selected *I–z* traces showing plateaus (longer than 0.02 nm) were used. Bias voltage: 100 mV, bin size: 25 pS (2.5 nA). (b) Conductance (triangle) and current (circle) values at the peak position in the conductance (current) histograms.

I–z traces for thiolated galactose measured with the 4MPBA tip

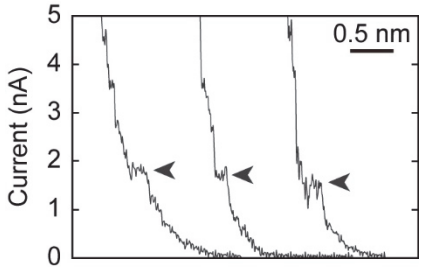

Fig. S4. Representative *I–z* traces measured with the 4MPBA tip and Au surface modified with thiolated galactose. Arrowheads indicate plateaus. Each plot is shifted horizontally for clarity. Bias voltage: 200 mV, initial set-point current: 7.5 nA.

Conductance histograms obtained with the 4MPBA-modified tip

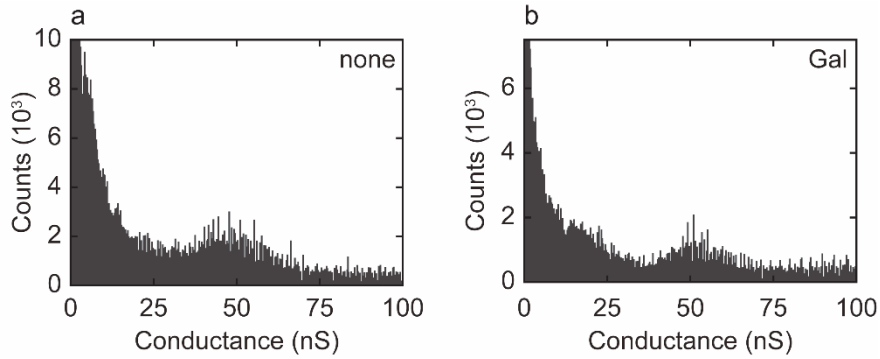

Fig. S5. Conductance histogram obtained using the 4MPBA-modified tip and Au substrate in (a) pure and (b) galactose solutions.

Proposed molecular model of 1:2 glucose–4MPBA junction

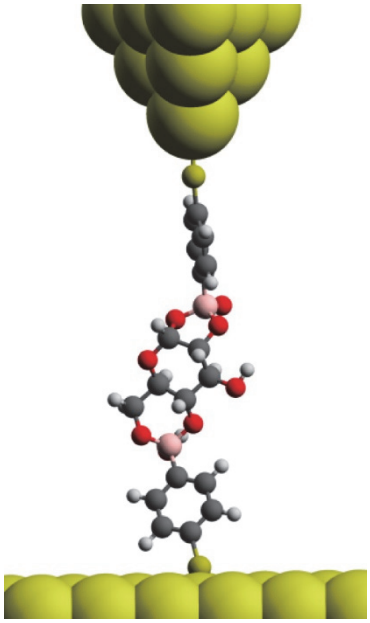

Fig. S6. The molecular moiety was optimized using B3LYP with the 6-31G* basis set. Color code: gray, carbon; white, hydrogen; red, oxygen; pink, boron; yellow (small spheres), sulfur; yellow (large spheres), gold.

Conductance histogram of 1:2 glucose-4MPBA supramolecular junction

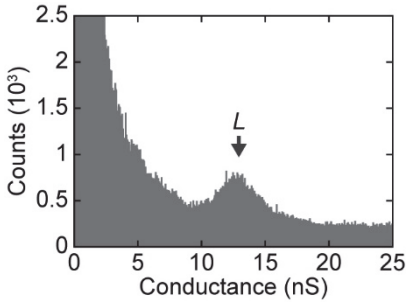

Fig. S7. A 1 nA/V preamplifier, more sensitive than a logarithmic preamplifier at small conductance region, was used. The *H* peak in Fig. 2c was out of the measurable range.

Single-molecule detection of glucose in artificial sweat

To confirm the applicability of the present method to biological samples, we measured glucose in artificial sweat. The artificial sweat was prepared with L-histidine (0.05% (w/v)), NaCl (0.5% (w/v)), and sodium hydrogen phosphate (0.5% (w/v)) according to the International Standard Organization (ISO105-E04). The glucose concentration was 0.1 mM, which is in the range of typical sweat glucose concentrations of hypoglycaemic and hyperglycaemic patients.[4] Current measurements were carried out in this solution using 4MPBA-modified tip and substrate. Plateaus found in the *I–z* traces (Fig. S8a) indicate the formation of the molecular junction. The conductance histogram constructed from those traces (Fig. S8b) showed two peaks at 55 nS (labeled "*H*") and at 13 nS ("*L*"). These peaks coincide with those observed in the buffer solution (52 nS and 13 nS, see Fig. 2), demonstrating that the *H* and *L* peaks originate from the 4MPBA dimeric molecular junction and 4MPA–glucose supramolecular junction, respectively. These results show that glucose single-molecule detection can be achieved in artificial sweat by the *L* peak, and imply the possibility of sweat-based glucose monitoring using the present methodology.

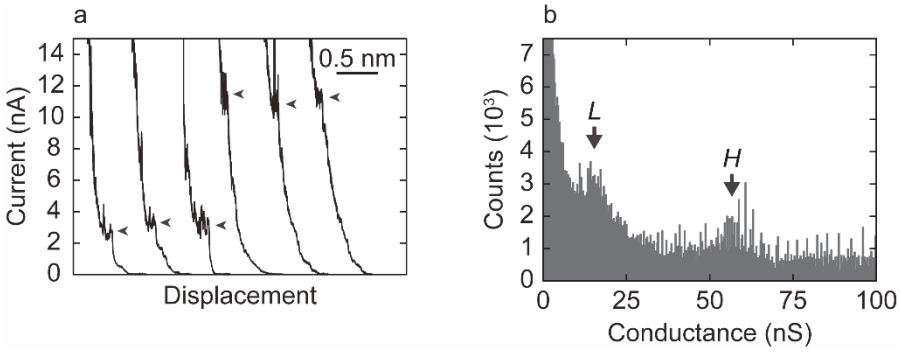

Fig. S8. (a) *I–z* traces and (b) conductance histogram obtained with glucose in artificial sweat using the 4MPBA-modified tip and Au substrate. Arrowheads and arrows indicate plateaus and peaks, respectively. Each *I–z* plot is shifted horizontally for clarity. Bias voltage: 200 mV, initial set-point current 100 nA. Bin size: 25 pS.

Cyclic voltammograms for the reductive desorption of thiol on a polycrystalline gold electrode

To confirm the chemisorption of sample thiols, i.e., thiolated glucose and 4MPBA, on a Au surface, we measured the reductive electrochemical desorption of the thiols (Fig. S9). Cathodic peaks originating from the thiol desorption were observed for both thiolated glucose and 4MPBA, demonstrating chemisorption of thiols on gold surfaces. Broad peaks observed for the 4MPBA-modified electrode were consistent with those observed in the reductive desorption of aromatic thiol.[5]

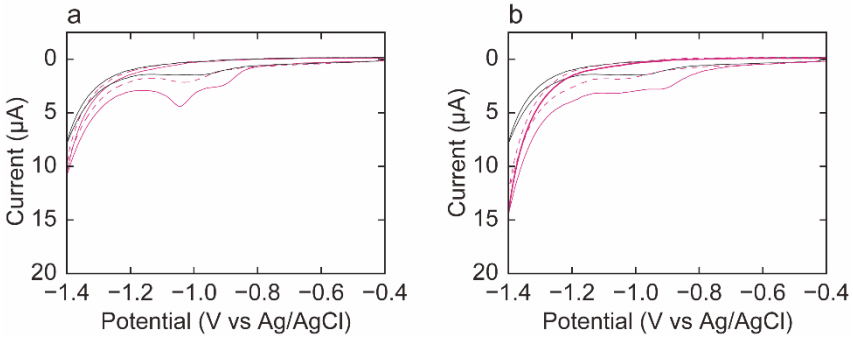

Fig. S9. Reductive desorption of thiol on a gold electrode (surface area: 2 mm^2). (a) thiolated glucose, (b) 4MPBA. (magenta) Au electrode modified in 50 μM ethanolic solution of thiol for 1 h. The first and second scans are shown as solid and dashed lines, respectively. (black) Bare gold electrode. Electrolyte: 0.1 M NaOH aqueous solution, scan rate: 100 mV s^{-1}, scanning range: −0.4 to −1.4 V.

X-ray photoemission spectroscopy measurement of 4MPBA on Au(111)

In addition to the electrochemical desorption (Fig. S9), X-ray photoemission spectroscopy (XPS) was used to confirm the chemisorption of 4MPBA on a gold surface. Fig. S10 shows the XPS spectra of sulfur (S 2p), boron (B 1s), and oxygen (O 1s) for the 4MPBA-modified Au(111) surface. Previous XPS studies of thiols on Au substrates have shown that the S 2p peaks consists of a doublet corresponding to the $2p_{1/2}$ and $2p_{3/2}$ peaks separated by 1.2 eV with a 2:1 area ratio.[6] Fitting the S 2p peaks (Fig. S10a) with this doublet revealed binding energies of 162.0 and 163.2 eV. These values are in agreement with those found for sulfur bound on gold.[7] The binding energies for free, unbound sulfur are 163.5 and 164.7 eV,[7] but these peaks were not observed in Fig. S10a. Thus, the S 2p spectrum demonstrates the chemisorption of the thiol. The B 1s photoelectron peak appeared at a binding energy of 190.8 eV (Fig. S10b), which is in accordance with that of boron in 4MPBA.[8] Furthermore, the O 1s binding energy was found to be 532.3 eV (Fig. S10c), which indicates the presence of the boronic acid group.[9] Taken together, the XPS data demonstrates the successful immobilization of 4MPBA on Au surfaces by chemisorption.

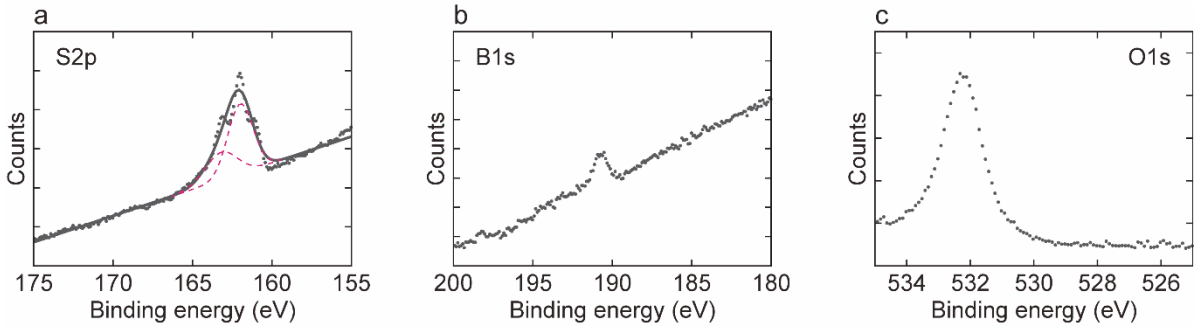

Fig. S10. XPS spectra of (a) S 2p, (b) B 1s and (c) O 1s regions of 4MPBA-modified Au surface. The S 2p spectrum (a) was deconvoluted by fitting the $2p_{1/2}$ and $2p_{3/2}$ doublet.

Experimental Procedures

Reagents. The reagents were of the highest grade available. Deionized water purified using a Milli-Q water purification system (Japan Millipore, Tokyo, Japan) was used for all experiments. Glucose and galactose derivatives containing a 2-mercaptoethyl linker were synthesized according to a previously reported procedure.[10]

Tip and sample preparation. Small pieces of a gold wire (0.25 mm diameter, 99.95%) were electrochemically etched in a 3 M NaCl in 1% perchloric acid at an AC voltage of 10 V.[11] The etched metal tips were insulated with poly(dimethylsiloxane) except for their very apices.[12] The insulated metal tips were immersed in a 7.5 mM ethanolic solution of 4MPBA for 12 h at room temperature. Full, or at least highly dense, monolayer formation is expected at the tips based on the concentration and immersion time.[13] The modified tips were thoroughly washed with ethanol and water and dried under a gentle stream of nitrogen prior to use.

Ultraflat gold films grown epitaxially on mica were used as Au(111) substrates (Fig. S11).[14] The gold substrates were immersed in a 50 μM ethanolic solution of either 4MPBA or thiolated monosaccharide derivatives for 1 h. The chemisorption of the thiols was confirmed by voltammetric reductive desorption (Fig. S9) and XPS (Fig. S10). Based on the selected concentration and immersion time, adlayer formation during the thiol adsorption process should be in the initial stages.[15] Thus, the concentration of sample molecules on the substrate surface should be low, which

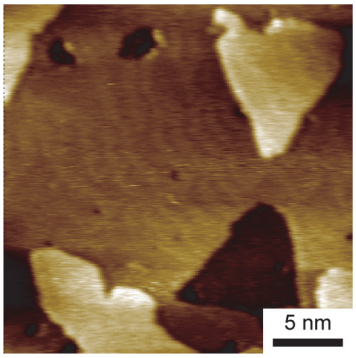

Fig. S11. STM image of ultraflat gold surface observed in air. Bias voltage: 0.4 V, set-point current: 0.5 nA.

reduces the possibility of the formation of multiple junctions. The substrates were washed with pure ethanol and blown dry with pure nitrogen. The substrate was then mounted on a sample cell of STM. The cell was filled with either a 10.0 mM monosaccharide solution in a 0.1 M HEPES buffer (pH 8.5) or pure 0.1 M HEPES buffer (pH 8.5).

Current Measurements. Tunneling current measurements were performed on an SPM 5100 system (Agilent Technologies, Santa Clara, CA). Platinum wires were used as the reference and counter electrodes, and the surface potential of the Au(111) substrate was maintained at its rest potential during measurement under potential control. Before current measurements, the STM instrument was stabilized according to a previous study[16] for suppressing the unwanted thermal drift of the STM scanner. The molecular tip was brought in close proximity to, but not in contact with, the sample surface by applying a high set-point current at a bias voltage of 200 mV under the STM feedback control. The bias voltage was selected to avoid the breakdown of the molecular junction and to ensure that the peak in the conductance histogram, arising from the electron transport through the junction, was distinct from the background at the low conductance region. The set-point values of 7.5 nA (1 nA/V preamplifier) and 100 nA (logarithmic preamplifier) were used for the surface-tethered and free monosaccharides, respectively. After a short delay time of 100 ms, the tip was pulled up at a velocity of 10 nm/s with the feedback loop of STM disabled, and *I*–*z* traces were recorded at a sampling frequency of 20 kHz using a data acquisition unit (SL1000, Yokogawa Electric Corporation). In the *I*–*t* measurements, the feedback loop was disabled for 1 s, and the current flowing between the molecular tip and the sample surface was recorded at the same sampling frequency.

Statistical data analysis. Current measurements were repeated using independently prepared tips and sample surfaces for ensuring reproducibility. For each sample molecule, at least three independent sample surfaces were used. Measurements were performed with six or seven molecular tips for each sample surface. In total, at least 20 tips were used for a given sample molecule. The reproducibility was confirmed by comparing conductance histograms obtained using every

independent sample surface. The relative standard deviations were found to be <5%. Conductance histograms were constructed from selected *I–z* traces with plateaus longer than 0.02 nm.[17] Approximately 10% of the measured *I–z* traces exhibited these plateaus; this ratio is comparable to that observed when alkanedithiol molecular tips were used for measuring the conductance change induced by the formation of a single covalent bond with an alkanedithiol sample.[16]

2D histograms were created according to a previous study[18] as follows. Using the 1D histogram, the current peaks and their widths were calculated to determine the minimum and maximal current values of the plateau. Then, the *I–z* traces were selected according to the reported criteria,[18] i.e., with a current plateau length longer than 0.02 nm and a slope greater (shallower) than –5 nA/nm. For each of the selected traces, the end of the current plateau was determined, and this point was set as the origin in the displacement axis. Finally, the 2D histograms were constructed using these traces.

References

1. G. Springsteen and B. Wang, *Tetrahedron*, 2002, **58**, 5291-5300.
2. W. Haiss, H. van Zalinge, S. J. Higgins, D. Bethell, H. Höbenreich, D. J. Schiffrin and R. J. Nichols, *J. Am. Chem. Soc.*, 2003, **125**, 15294-15295.
3. W. Haiss, R. J. Nichols, H. van Zalinge, S. J. Higgins, D. Bethell and D. J. Schiffrin, *Phys. Chem. Chem. Phys.*, 2004, **6**, 4330-4337.
4. J. Moyer, D. Wilson, I. Finkelshtein, B. Wong and R. Potts, *Diabetes Technol. Ther.*, 2012, **14**, 398-402.
5. R. R. Kolega and J. B. Schlenoff, *Langmuir*, 1998, **14**, 5469-5478.
6. D. G. Castner, K. Hinds and D. W. Grainger, *Langmuir*, 1996, **12**, 5083-5086.
7. P. E. Laibinis, G. M. Whitesides, D. L. Allara, Y. T. Tao, A. N. Parikh and R. G. Nuzzo, *J. Am. Chem. Soc.*, 1991, **113**, 7152-7167.
8. D. Barriet, C. M. Yam, O. E. Shmakova, A. C. Jamison and T. R. Lee, *Langmuir*, 2007, **23**, 8866-8875.
9. R. I. Carey, J. P. Folkers and G. M. Whitesides, *Langmuir*, 1994, **10**, 2228-2234.
10. N. Skirtenko, M. Richman, Y. Nitzan, A. Gedanken and S. Rahimipour, *Chem. Commun.*, 2011, **47**, 12277-12279.
11. D. Gingery and P. Buhlmann, *Rev. Sci. Instrum.*, 2007, **78**, 113703.
12. M. Kuroda and T. Nishino, *Rev. Sci. Instrum.*, 2011, **82**.
13. A. Ulman, *Chem. Rev.*, 1996, **96**, 1533-1554.
14. P. Wagner, M. Hegner, H. J. Guntherodt and G. Semenza, *Langmuir*, 1995, **11**, 3867-3875.
15. C. D. Bain, E. B. Troughton, Y. T. Tao, J. Evall, G. M. Whitesides and R. G. Nuzzo, *J. Am. Chem. Soc.*, 1989, **111**, 321-335.
16. T. Nishino, *Chemphyschem*, 2010, **11**, 3405-3407.
17. P. T. Bui, T. Nishino, Y. Yamamoto and H. Shiigi, *J. Am. Chem. Soc.*, 2013, **135**, 5238-5241.
18. M. Frei, S. V. Aradhya, M. Koentopp, M. S. Hybertsen and L. Venkataraman, *Nano Lett.*,

2011, **11**, 1518-1523.